Numerical Study on Combustion Stability of n-Heptane /Air in a Micro Tube Combustor

LI Junwei, WEI Zhijun, WANG Ningfei
School of Aerospace Engineering
Beijing Institute of Technology, Beijing 100081, P.R.China

1 Introduction

Currently, with the rapid development and application of portable electronic devices and micro electromechanical systems (MEMS), an urgent demand for a higher energy density, replenish energy efficient portable power supply is put forward to their batteries. Micro power-generating system will probably replace traditional chemical battery and become the most promising and potential miniature power device[1]. Combustion technology in a micro space is still faced with some special difficulties. In order to solve the difficulties faced by liquid fuel combustion in micro combustors, various means are proposed by researchers[2,3].

Spray is one way to make liquid fuel fast evaporate[4-6]. However, combustion rate of liquid fuel with air in combustion chamber is dominated by evaporation rate and mixing rate. In a micro burner, due to limited mixing and reaction space, spray combustion feature is different from that in a traditional burner. To better understand spray combustion characteristics in a micro burner, two burners are numerically studied.

2 Physical Model

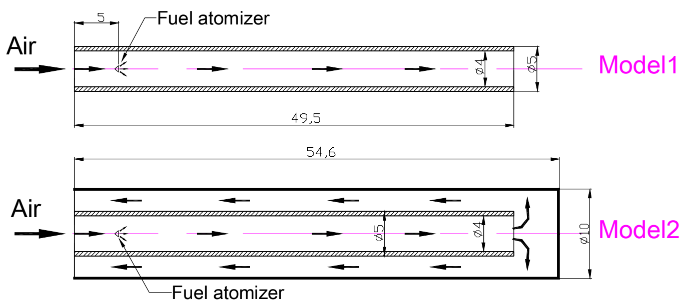

Figure 1 Schematic of two tube burners

Figure 1 shows a schematic diagram of two tube burners. Model1 is a tube burner without preheating and Model2 has an outer tube to recover heat in the exhausts. The dimensions of the small tube are 4 mm in inner diameter and 49.5 mm in length. The outer tube in Model2 is 10 mm in inner diameter. A pressure atomizer is used in the combustor, from which liquid n-heptane is sprayed. The combustion air is injected into the inner tube through air inlet nozzle. The combustion products are expelled from the inner tube in Model1 and from the outer annular chamber in Model2.

3 Numerical Method

A two-dimensional axi-symmetric model is employed to capture thermal gradients of the gas domain in the axial and transverse directions. The commercial CFD package Fluent 6.3 is used to solve the steady state Navier-Stokes and energy equations for the convecting fluid coupled with the energy equation for the solid wall using a finite volume method. Structured grids are employed in the computational domain and the grid number is about 50,000. Grid-independence of the results was verified.

Since velocity of the hot products are accelerated and the maximum is up to about 15m/s, Reynolds number maybe as high as 2511, which is in the regime of turbulent flow. Therefore, standard k-e model and eddy dissipation model has been adopted to model turbulent combustion.

The single-step reaction of heptanes and air is employed in order to simplify the complex combustion. The activation energy and frequency factor used here are E=70.29 kJ/mole and A =2.2e+8 m3/mole/s, respectively. DO(Discrete Ordinate) radiation model has been adopted in consideration of the gas phase as a gray absorbing emitting medium. All gas and solid-phase thermodynamic and transport properties are modeled as temperature dependent using handbook values. The wall is made of stainless steel, and its thermal conductivity is 16.3W/m-K

Following boundary conditions are used in the simulation. Mass flow rate condition is applied to air flow entrance. No-slip condition and zero diffusive flux condition are applied to coupled wall between fluid and solid. To minimize the computational intensity, an axis boundary condition is used along the central chamber and half of the system is modeled. One atmosphere is prescribed at the burner exit. In all burners studied, heat transfer coefficient of the outer wall is varied and heat loss on combustion stability is studied.

In the following study, n-heptane flow rate of 1mg/s is fixed, and the droplet diameter is 1 μ m. The Discrete Phase model of FLUENT has been exploited to model the droplet phase. Trajectories of droplets are computed in a Lagrangian frame. Droplets can exchange heat, mass, and momentum with the continuous gas phase by vaporization model.

4 Results and Discussions

4.1 Effects of Equivalence Ratios on Flame Stability

For a fixed n-heptane flow rate, if air flow rate is varied, flame positions at various equivalence ratios can be obtained.

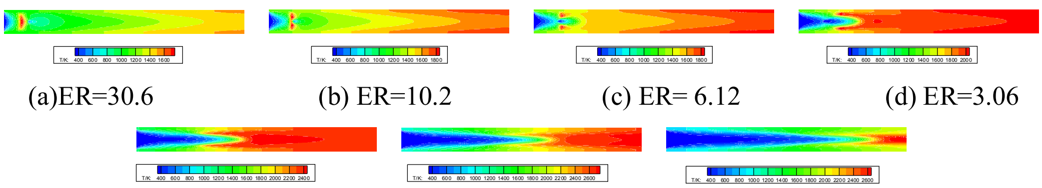

(a)ER=30.6 (b) ER=10.2 (c) ER= 6.12 (d) ER=3.06

(e)ER =1.53 (f)ER=1.02 (g)ER=0.77

Figure 2 Temperature contours for various Equivalence Ratios in Model1

It is shown in Figure 2 that the flame moves with variation of equivalence ratios. When ER is greater than 10.2, the flame is located upstream of n-heptane injector. This is due to significant excess of n-heptane. Under the effects of molecular diffusion, gasified n-heptane molecules move upstream, and react with the incoming air. In this case, combustion heat release is very small, and the maximum flame temperature is only 1800K. With the increase of air flow, combustion heat release increases and the maximum flame temperature is up to

2700K, which is much higher than the adiabatic flame temperature (about 2270 K). This result could be due to the use of a single step global reaction which cannot account for dissociation and partial fuel oxidation. But in the cases of large air flow, flame is stretched longer, which reduces thermal feedback through the wall. Finally, flame will be blown out.

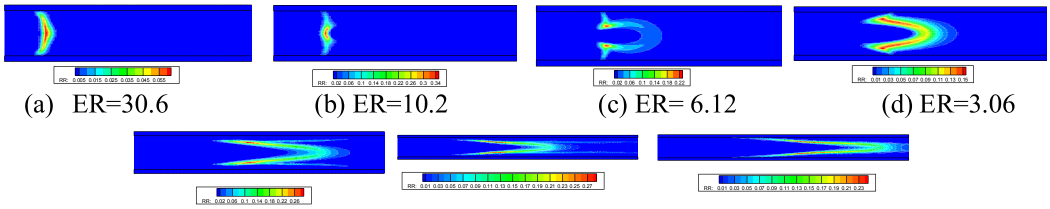

(a) ER=30.6 (b) ER=10.2 (c) ER= 6.12 (d) ER=3.06

(e)ER =1.53 (f)ER=1.02 (g)ER=0.77

Figure 3 Reaction rate contours for various ER in Model1

Figure 3 shows reaction rate contours in Model1. With increase of equivalence ratio, reaction zone is moving from the entrance to the exit. When air flow velocity is low, the flame is mainly located in the vicinity of the fuel injector and its length is very short. With the increase of air flow, the flame is stretched and its length increases. When ER is 0.77, flame becomes the longest. If much more air is injected, part of the flame will move out of the tube and extinguishment will occur.

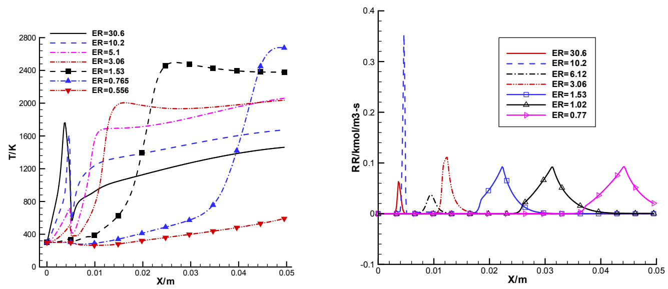

Figure 4 Axial centerline temperature and reaction rate distributions in Model1. Left: Temperature distribution. Right: Reaction Rate distribution.

Left figure in Figure 4 shows temperature distribution along the axis for various equivalence ratios. In the case of ER greater than 3.06, a temperature peak appears on the axis near the fuel injector. After the peak, temperature gradually increases along the axis. With decrease of ER from 30.6 to 3.06, the peak temperature decreases from 1800K to 500K. The reason is that with the increase of air flow, the reaction zone moves from a position on the axis ahead the fuel injector to a position on both sides of the injector. As the air flow is further increased, the reaction moves downstream the injector.

Right figure in Figure 4 shows reaction rate distribution on the axis. It can be seen that with decrease of ER, the maximum reaction rate position gradually moves downstreams. When ER larger than 10.2, the reaction zone is ahead the fuel injector. In the case of ER smaller than 10.2, the reaction zone is blown downstream. If ER becomes much smaller, the maximum reaction rate on the axis is essentially equal.

4.2 Effect of heat recovery on flame stability

In order to understand effect of heat recovery on flame stability, numerical simulations for Model2 at various equivalence ratios are carried out. The outer wall of Model2 is not adiabatic and the heat loss coefficient is set to 10 W/m^2-K.

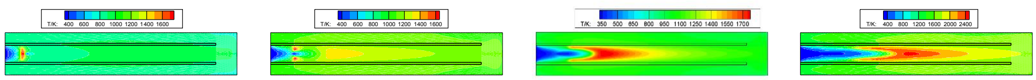

(a)ER=15.3 (b) ER=6.12 (c) ER= 3.06 (d) ER=1.02

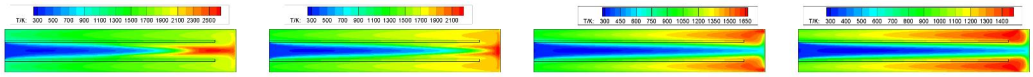

(e) ER=0.7 (f)ER=0.51 (g) ER =0.38 (h) ER =0.31

Figure 5 Temperature contours for various equivalence ratios in Model2

Temperature contours for various equivalence ratios in Model2 are shown in Figure 5. It can be seen from the figures that the reaction zone moves with variations of equivalence ratios. Even though there is heat transfer between Model2 and the surroundings, Model2 can still steadily operate in the equivalence ratio range from 15.3 to 0.31, which is wider than that of Model1 with an adiabatic outer wall. However, fuel-rich limit of Model2 is smaller than that of Model1 without heat loss. This is because the outside wall of the inner tube in Model2 is not adiabatic and the exhausts would take away heat from it. In contrast, in Model1, the transferred heat from the flame to the tube wall is entirely used to preheat the incoming gas. In addition, at ER of 0.77, due to high-speed air flow, diffusion flame in Model1 is blown out. While in Model2, its fuel-lean limit is up to 0.31. This could attribute to that in Model2, changing of flow direction reduces gas flow velocity and plays a role in stabilizing the flame.

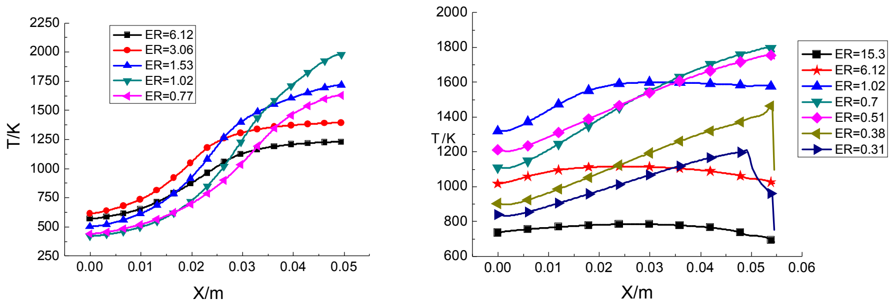

(a) Model1 (b) Model2

Figure 6 Axial outer wall temperature distributions

Figure 6 shows axial outer wall temperature distributions in two burners at heat loss coefficient of 10W/m^2-K. It can be seen from the figure that there is a large temperature gradient along the tube wall in Model1, hot exit wall and cold entrance wall. When equivalence ratio is 1, the outer wall temperature varies from 300K to 2000K. This indicates that hot exhausts cannot heat the unburned gases to a high temperature. On the contrary, in Model2, the outside wall temperature is uniform along the axis. The maximum temperature gradient occurs at ER of 0.7, with temperature variation from 1100K to 1800K. It can be estimated from the outer wall temperature that the inner tube wall temperature is high and uniform, which is advantageous to flame stabilization.

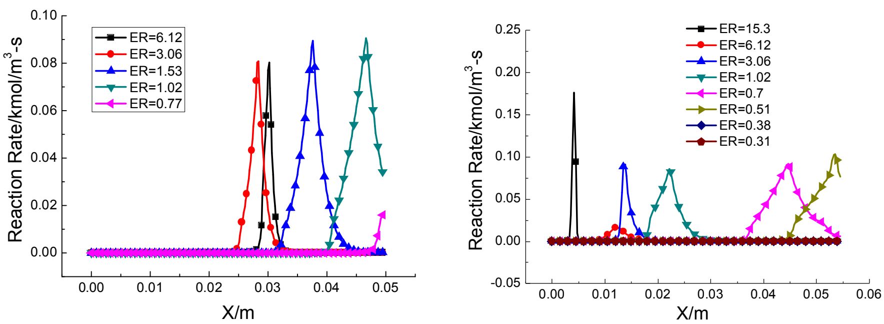

(a) Model1 (b) Model2

Figure 7 Axial centerline reaction rate distributions

Figure 7 shows that when the heat loss coefficient is 10 W/m^2-K, for the same equivalence ratio, flame position in Model1 is closer to the tube exit than that in Model2. When equivalence ratio equals 3.06, flame in Model1 is located at 0.027mm, while the flame in Model2 is located at 0.014mm. With the increase of equivalence ratio, the flame moves down streams. For ER of 0.77, the flame in Model1 is at the exit, while in Model2 the flame is still located at 0.045mm.

4.3 Effect of Heat loss on flame stability

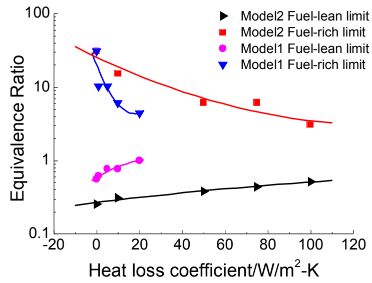

Figure 8 Flammable limits of two burners at different heat loss coefficients

Figure 8 shows effects of heat loss coefficients on flammable limits of two burners at ER equal to 1. It can be seen from the figure that with increase of the heat loss coefficient, the flammable limit of Model1 rapidly narrows down. When the heat loss coefficient is greater than 30W/m^2-K, stable combustion of n-heptane and air cannot be sustained. While for Model2, with increasing the heat loss coefficient, the flammable limit is gradually narrowing. Even when the coefficient is larger than 100 W/m^2-K, the burner can still work. In addition, if there is no heat loss in both burners, fuel-rich limit in Model1 is slightly larger than that in Model2 because of heat loss from the inner wall in Model2. However, the fuel-lean limit of Model2 is less than that of Model1 all along. It is because larger air flow rate will result in the flame in Model1 more likely to be blown out.

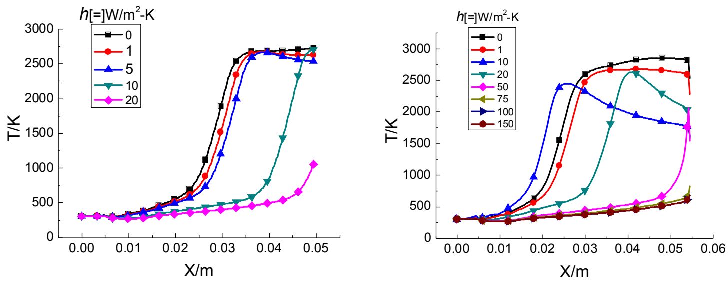

(a) Model1 (b)Model2

Figure 9 Axial centerline temperature distributions for various heat loss coefficients

Figure 9 shows that with increasing heat loss coefficients, the temperature on the axis in both burners gradually decreases, and the location of the flame moves downstream. When the heat loss coefficient is 20 W/m^2-K, the maximum temperature on the axis in Model1 is only 1000K, while the temperature in Model2 is about 2500K. Additionally, if the heat loss coefficient is greater than 75 W/m^2-K, the axial temperature distribution in Model2 coincides with that for the heat loss coefficients of 75 W/m^2-K. This indicates that the flame is blown downstream and the combustion zone is not in the tube center.

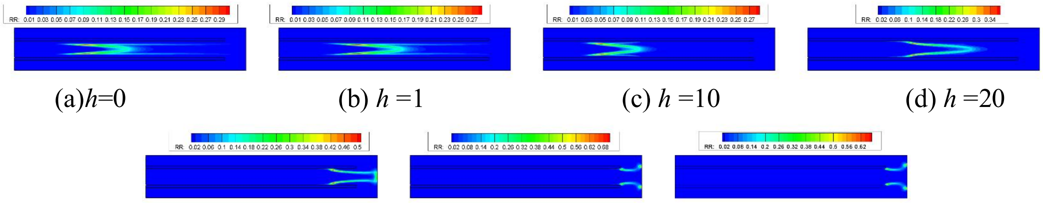

(a) h=0 (b) h =1 (c) h =10 (d) h =20

(e) h =50 (f) h =75 (g) h =100

Figure 10 Reaction rate contours for various heat loss coefficients of Model2 at ER=1.02(h Unit: W/m^2-K)

Figure 10 clearly indicates that the reaction zone moves with the variations of heat loss coefficients. With increasing heat loss coefficients, the reaction zone gradually moves downstream and its shape is also changing, from “U” shape at low heat loss coefficient to “π ”shape at high heat loss coefficient. Finally, the flame moves to the bottom of the outer tube in Model2. This is due to the fact that with the increase of heat loss coefficients, wall temperature of the inner tube decreases, and the preheated temperature of unburned gases decrease, leading to movement of the flame.

5 Conclusions

(1) For a tube burner without heat recovery, the location and temperature of diffusion flame change with the air velocity and heat loss coefficient. If there is a large air flow rate or heat loss coefficient, the flame would be blown out of the tube.

(2) For a tube burner with heat recovery, it can stably work at a larger air flow rate and high heat loss coefficient. But the position and shape of the flame may change.

(3) With the increase of heat loss coefficient, the flammable limits of the latter are much larger than that of the former. This is due to the fact that hot exhausts preheat the unburned gas through the inner tube wall and the flame stability is enhanced.

References

[1] Maruta K. (2011). Micro and mesoscale combustion. Proc. Combust. Inst. 33: 125-150.

[2] Sadasivuni V, Agrawal AK. (2009). A novel meso-scale combustion system for operation with liquid fuels. Proc. Combust. Inst. 32: 3155–3162.

[3] Li YH, Chao YC, Dunn-Rankin D. (2006).Combustion in a meso-scale liquid-fuel-film combustor with central-porous fuel inlet. Combust. Sci. and Tech. 180:1900-1919.

[4] Deng W., Klemic JF, Li X. (2007). Liquid fuel micro-combustor using micro-fabricated multiplexed electro-spray sources. Proc. Combust. Inst. 31: 2239–2246.

[5] Russo S, Gomez A. (2006). Physical characterization of laminar spray flames in the pressure range 0.1–0.9 MPa. Combustion and Flame, 145:339–356.

[6] Mattioli R, Pham T K, Dunn-Rankin D. (2009). Secondary air injection in miniature liquid fuel film combustors. Proc. Combust. Inst. 32:3091-3098.